05,13

Spin magnetoresistance of a strontium iridate/manganite heterostructure

© K.Y. Constantinian[1], G.A. Ovsyannikov[1], A.V. Shadrin[1,2], V.A. Shmakov[1], A.M. Petrzhik[1], Yu.V. Kislinskii[1], A.A. Klimov[1,3]

[1] Kotelnikov Institute of Radio Engineering and Electronics, Russian Academy of Sciences, Moscow, Russia
[2] Moscow Institute of Physics and Technology (National Research University), Dolgoprudny, Moscow Region, Russia
[3] MIREA — Russian Technological University, Moscow, Russia

E-mail: karen@hitech.cplire.ru

Received April 29, 2022
Revised April 29, 2022
Accepted May 12, 2022

The results of the angular dependences of the magnetoresistance of the $SrIrO_3/La_{0.7}Sr_{0.3}MnO_3$ heterostructure made of oxide thin films epitaxially grown on a $NdGaO_3$ substrate are presented and discussed. The resistance of the heterostructure was measured in configuration of planar Hall effect with magnetic field applied in parallel making possible to estimate the spin-Hall angle. The contribution of the anisotropic magnetoresistance and the spin-Hall magnetoresistance occurred due to strong spin-orbit interaction in the $SrIrO_3$ film were evaluated.

Keywords: strontium iridate, spin-orbit interaction, spin magnetoresistance, spin-Hall angle.

DOI: 10.21883/PSS.2022.10.54227.46HH

1. Introduction

Charge transport is a key physical mechanism of modern solid-state electronics, in the development of which spin-dependent processes occurring at interfaces in heterostructures are becoming increasingly important. The dynamics of the generation and transport of the spin current in heterostructures rapidly acquires a decisive importance for the operation of the entire device. Thus, in a heterostructure with an interface of a ferromagnet and a material with strong spin-orbital coupling (SOC), due to the direct and inverse spin Hall effects, it becomes possible to convert the charge current into spin and vice versa [1] with high efficiency (see, for example, [2]). In the works [3,4] it was reported about the appearance of a pure spin current I_S in the oxide heterostructure $SrIrO_3/La_{0.7}Sr_{0.3}MnO_3$ (SIO/LSMO) at ferromagnetic resonance (FMR) and about the registration of the charge current I_e on the electrically conductive SIO film due to the transformation of I_S into I_e due to the inverse spin Hall effect. The study of the characteristics of spin magnetoresistance R_{SMR} [1] can be successful in estimating the value of the spin Hall angle θ_{SH}, but the problem is complicated by the presence of anisotropic magnetoresistance R_{AMR} [5], which has an angular dependence similar to the R_{SMR} with 2φ-periodicity [1,6]. It should be noted that in structures with strong SOC, the contribution of the Rashba–Edelstein magnetoresistance R_{RE} can be noticeable due to magnetoelectric effects [7,8]. Differences in the $R_{\mathrm{AMR}}(H)$ and $R_{\mathrm{SMR}}(H)$ dependences of the magnetoresistance can be found by comparing the characteristics for the SIO/LSMO heterostructure and the LSMO film. In this work, the magnetoresistances of both structures epitaxially-deposited on a $NdGaO_3$ substrate will be discussed. Measurements of the magnetoresistance (MR) were carried out in a 4-point configuration with a magnetic field in the plane of the substrate.

2. Heterostructures and measurement procedure

Thin films of SIO (of a few nm in thickness) and LSMO (of tens nm) were deposited on (110) $NdGaO_3$(NGO) single-crystal substrates. Epitaxial film growth was carried out by magnetron sputtering at substrate temperatures of 770–800°C in a mixture of Ar and O_2 gases at pressure of 0.3 mBar [3]. The diffraction patterns of the heterostructures showed multiple reflections from the (001) SIO and (001) LSMO planes, coinciding in direction with reflections from the (110) NGO substrate plane, which corresponds to the growth of „cube on cube": (001) SIO ‖ (001) LSMO ‖ (110)NGO and [100] SIO ‖ [100] LSMO ‖ [001] NGO.

Scheme for setting of current I, magnetic field H and measurement of voltage V, proportional to magnetoresistance $R(H)$ on the heterostructure with width $w = 0.1$ mm and distance $L = 0.6$ mm between potential contacts, is shown in Fig. 1.

The $R(H)$ measurements were performed at room temperature 300 K in magnetic field lying in the $X-Y$ plane. An alternating current with an amplitude of $I = 0.5$ mA at a frequency of $F \approx 1$ kHz was set, and a voltage V proportional to MR was measured by a lock-in amplifier. Measurements of the angular dependences of MR $R(\varphi)$

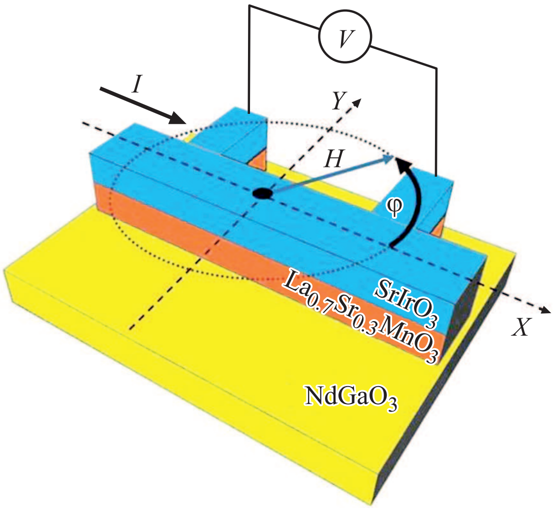

Figure 1. SIO/LSMO heterostructure on (110) NGO substrate and the 4-point measurement scheme. The field H rotated in the plane, forming an angle φ relative the direction of current flow I.

were carried out by rotating the substrate relative to the direction of the field H given by Helmholtz coils. When measuring the MR, the magnetic field was swept in the sequence: $0 \to H_+ \to H_- \to 0$ with a step of $\Delta H = H_{MAX}/N$, $N = 200{-}1500$, $H_+ = H_{MAX}$, $H_- = -H_{MAX}$. Note that we measured the longitudinal MR and extracted data on the resistivity, which is proportional to the number of squares $L/w = 6$ of the structures (one square corresponds to a film section of 100×100 microns). The static magnetic characteristics $M/M_S(H)$ were measured using a unit for the longitudinal magnetooptical Kerr effect (MOKE).

In order to minimize the change in temperature T of the sample under study due to heating of the coil during the recording of the track, the integration time constant of the lock-in amplifier was set to $\tau = 30$ ms, and the temperature difference ΔT of the start and finish of the recording, measured with a relative accuracy up to 5th significant character, was $\Delta T < 0.3$ K, which made it possible to correct the final dependences $R(H)$ on resistances R_0 at $H = 0$.

3. Measurement results and discussion

The magnetic field dependences of the normalized magnetization M/M_S of the LSMO film and the SIO/LSMO heterostructure measured with the MOKE are shown in Fig. 2. The easy LSMO magnetization axis in Fig. 2, *a* corresponds to the hysteresis curve (*1*), the hard axis corresponds to (*2*). In Fig. 2, *b*, the hysteresis dependences of SIO/LSMO are taken at an angle of 45° relative to the edge of the substrate for the easy axis (1) and 170° (2) relative to the hard axis. It can be seen that the saturation field in both cases is $H_S \approx 100$ Oe.

Figure 3 shows the $R(H)$ dependences for the LSMO film and the SIO/LSMO heterostructure. The thickness of the LSMO films was equal to 50 nm in both cases, and the thickness of the SIO film in the heterostructure was $d = 10$ nm. Figure 3 shows the corrected dependences $R(H)$, which take into account heating, as evidenced by the coinciding (within noise limits) normalization value R_0 when passing through $H = 0$. On the SIO/LSMO heterostructure, MR ΔR jumps were observed, which, depending on the angle φ, occurred both in the direction of increasing R and decreasing. There were no MR jumps on the LSMO film. It should also be noted that when a magnetic field perpendicular to the plane of the substrate was set under conditions similar in field H, no change in MR was observed.

Figure 4 shows the angular dependences of the change in the MR of the LSMO film and the SIO/LSMO heterostructure, normalized to R_0, corresponding to the field $H_{MAX} = 91$ Oe. For cases in which the jump on the SIO/LSMO occurred at $H < H_{MAX}$, in order to eliminate the effect of jumps on the amplitude R, linear extrapolation

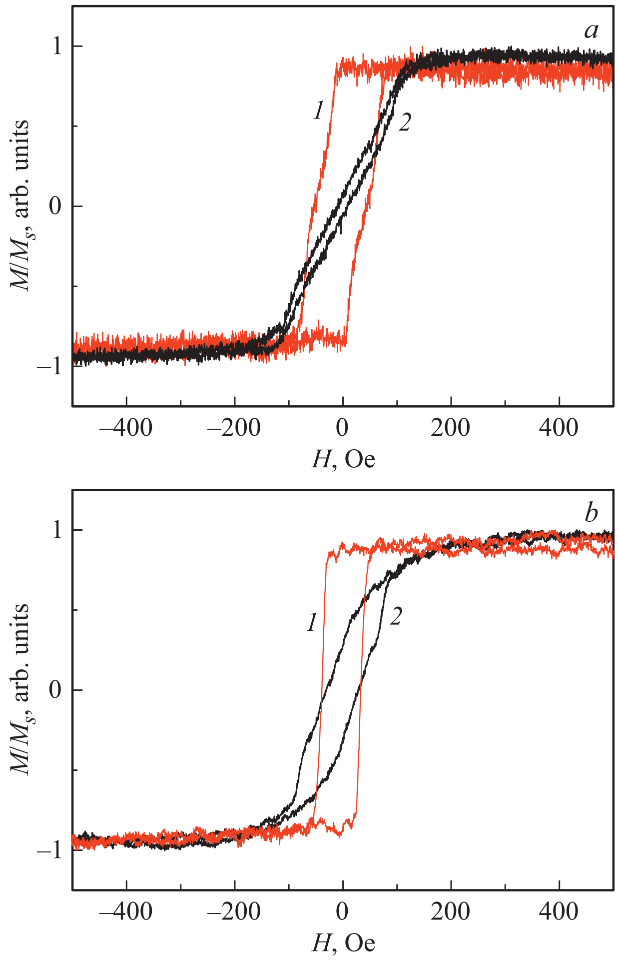

Figure 2. The dependences of the normalized magnetization measured using the magnetooptic Kerr effect, the curves (*1*) correspond to the easy magnetization axis, (*2*) correspond to the hard axis. (*a*) LSMO film, (*b*) SIO/LSMO heterostructure, easy axis (*1*) is at an angle 45° relative to the edge substrates, hard axis (*2*) is at an angle 170°.

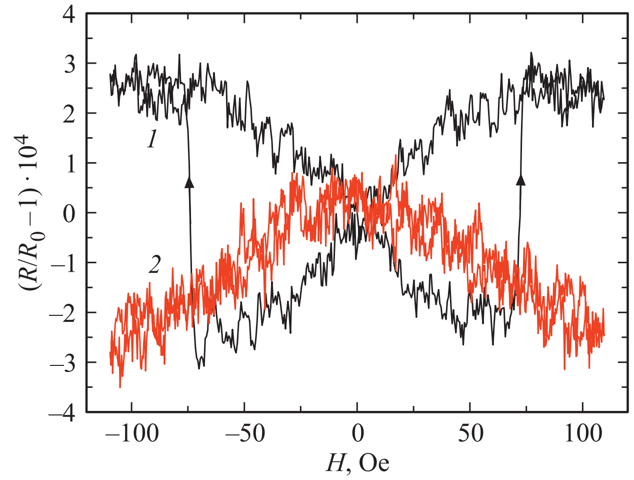

Figure 3. Dependence of the normalized MR on H for a SIO/LSMO heterostructure ($R_0 = 9.4034$ in measured voltage units V) taken at an angle $\varphi = 55°$ with respect to the current setting (*1*) and MS of the LSMO film ($R_0 = 7.3334$) taken at $\varphi = 50°$ (*2*). The arrows show the directions of jumps R. The direction of the easy magnetization axis with respect to the current I was an angle 45°.

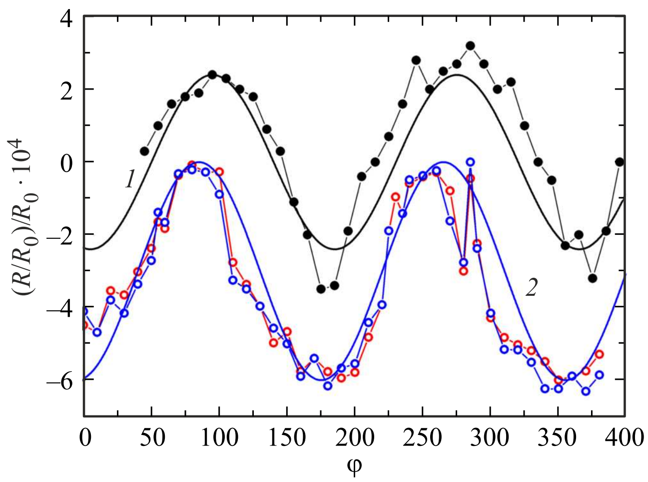

Figure 4. Angular dependences of the normalized amplitudes of the MR for LSMO film (*1*) and the SIO/LSMO (*2*) heterostructure. Experiment — symbols, approximations (*1*) and (*2*) are drawn by functions $\sin(2\varphi)$ — solid lines. Experimental data for LSMO are shifted to the right with respect to $\varphi = 0$ with a 50° phase shift. For SIO/LSMO, the symbols corresponding to the $H = +90$ Oe field are filled in red, filled in blue — corresponding to the $H = -90$ Oe.

was applied over the section $R(H)$ before the jump and the data shown in the figure correspond to $R/R_0 < 1$. It can be seen from Fig. 4 that the angular dependences of the MR of the SIO/LSMO heterostructures and the LSMO film are significantly different. The MR of an LSMO film is described by the known angular dependence of the anisotropic magnetoresistance $R_{\mathrm{AMR}}(\varphi) \sim R_0 + \Delta R \sin(2\varphi)$, where the component R_0 is independent of φ component. MR of the SIO/LSMO heterostructures except for $R_{\mathrm{AMR}}(\varphi)$ contains $R_{\mathrm{SMR}}(\varphi)$ connected in parallel and, what is important, is shifted to the region of negative values. The amplitude value of ΔR_{SMR} looks like [9]:

$$\Delta R_{\mathrm{SMR}}/R_0 \approx -(\lambda_S/d_{\mathrm{SIO}})AB\,\theta_{\mathrm{SH}}^2, \tag{1}$$

where

$$A = (1 + \rho_{\mathrm{SIO}} d_{\mathrm{LSMO}}/\rho_{\mathrm{LSMO}} d_{\mathrm{SIO}})^{-1},$$

$$B = G_{R\uparrow\downarrow} 2\rho_{\mathrm{SIO}}\lambda_S (1 + G_{R\uparrow\downarrow} 2\rho_{\mathrm{SIO}}\lambda_S)^{-1},$$

$G_{R\uparrow\downarrow}$ is real part of spin mixing conductance, specific values of resistance ρ and film thicknesses d are given for LSMO and SIO with corresponding indices, λ_S is spin diffusion length in SIO. To estimate the θ_{SH} parameter from the MR data of the SIO/LSMO heterostructure according to [4] for the SIO/LSMO boundary, the parameter $G_{R\uparrow\downarrow} \approx 10^{15}\,1/\Omega\cdot\mathrm{cm}^2$ for $d_{\mathrm{SIO}} = 10$ nm (as in our case) and for $\lambda_S = 1.4$ nm [10], $A = 2.6$ from $\rho_{\mathrm{SIO}} = 3\cdot 10^{-4}\,\Omega\cdot\mathrm{cm}$, $\rho_{\mathrm{LSMO}} = 9\cdot 10^{-4}\,\Omega\cdot\mathrm{cm}$ at $T = 300$ K from the amplitude value $\Delta R_{\mathrm{SMR}} = -6\cdot 10^{-4}$ (Fig. 4) we obtain the estimate $\theta_{\mathrm{SH}} \approx 0.35$, which exceeds the values of θ_{SH} for structures with Pt metal film [2,11].

Figure 5 shows the angular dependences of the resistance jump $\Delta R/R_0$ of the SIO/LSMO heterostructure, and the values of the magnetic field H of the beginning of the jump according to the data in the range of fields $H < 0$. Jumps were also observed at $H > 0$, and we do not associate the occurrence of jumps with the hysteresis M/M_S. It can be seen that jumps appear already at fields noticeably lower than the hysteresis value and appear only after the deposition of the upper SIO film. Although the nature of the jumps is not quite clear, but according to the theoretical model [12] in the case of a strong SOC in thin-film magnetic heterostructures, the possibility of a sharp increase in the mobility of domain walls arises, which can explain the appearance of jumps of MR on the SIO/LSMO heterostructure, geometry of which coincides with that

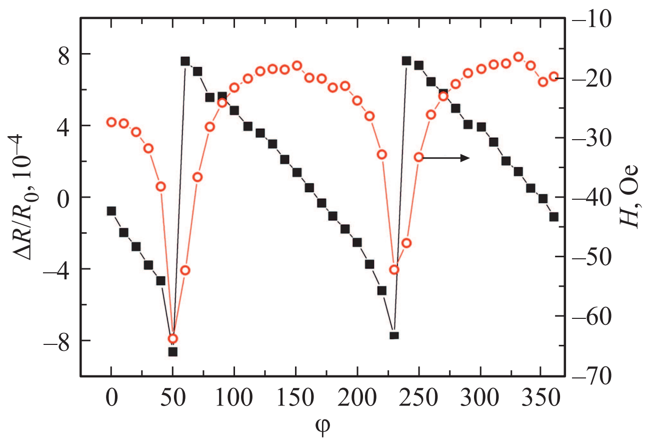

Figure 5. Angular dependences of the normalized jump amplitudes $\Delta R/R_0$ (squares) and their positions in the field H (circles) of the SIO/LSMO heterostructure.

considered in the model. Accordingly, in the case of a strong SOC, the θ_{SH} value may contain the R_{RE} component [12], which requires a separate study to evaluate.

4. Conclusion

Experimental study was made of the angular dependences of the $SrIrO_3/La_{0.7}Sr_{0.3}MnO_3$ heterostructures and the $La_{0.7}Sr_{0.3}MnO_3$ film at setting the magnetic field in the plane of the substrate. Only anisotropic magnetoresistance was observed on the $La_{0.7}Sr_{0.3}MnO_3$ film. For the $SrIrO_3/La_{0.7}Sr_{0.3}MnO_3$ heterostructure, the amplitude $\Delta R_{SMR}/R_0$ of the sinusoidal dependence of the spin magnetoresistance on the angle between the direction of the magnetic field and flowing current, the value of the spin Hall effect angle is estimated, which significantly exceeds the values of θ_{SH} for the Pt/LSMO heterostructure.

Acknowledgments

The authors would like to thank T.A. Shaikhulov for preparation of thin films and heterostructures.

Funding

This study was carried out under the sate assignment of the Kotelnikov Institute of Radio Engineering and Electronics of the RAS. The studies were performed using the equipment of the Unique Scientific Facility No. 352529 „Cryointegral“ (Agreement of the Ministry of Education and Science No. 075-15-2021-667).

Conflict of interest

The authors declare that they have no conflict of interest.

References

[1] Y.-T. Chen, S. Takahashi, H. Nakayama, M. Althammer, Sebastian T.B. Goennenwein, Eiji Saitoh, Gerrit E.W. Bauer. J. Phys.: Condens. Matter **28** 103004 (2016).
[2] Y. Du, H. Gamou, S. Takahashi, S. Karube, M. Kohda, J. Nitta. Phys. Rev. Appl. **13**, 054014 (2020).
[3] G.A. Ovsyannikov, T.A. Shaikhulov, K.L. Stankevich, Yu. Khaydukov, N.V. Andreev. Phys. Rev. B **102**, 144401 (2020).
[4] X. Huang, S. Sayed, J. Mittelstaedt, J. Mittelstaedt, S. Susarla, S. Karimeddiny, L. Caretta, H. Zhang, V.A. Stoica, T. Gosavi, F. Mahfouzi, Q. Sun, P. Ercius, N. Kioussis, S. Salahuddin, D.C. Ralph, R. Ramesh. Adv. Mater. 2008269 (2021).
[5] M. Ziese, S.P. Sena. J. Phys.: Condens. Matter 10, 2727 (1998).
[6] M. Althammer, S. Meyer, H. Nakayama, M. Schreier, S. Altmannshofer, M. Weiler, H. Huebl, S. Geprags, M. Opel, R. Gross, D. Meier, C. Klewe, T. Kuschel, J.-M. Schmalhorst, G. Reiss, L. Shen, A. Gupta, Yan-Ting Chen, G.E.W. Bauer, E. Saitoh, S.T.B. Goennenwein. Phys. Rev. B **87**, 224401 (2013).
[7] V.M. Edelstein. Solid State Commun. **73**, 233 (1990).
[8] J.C. Rojas Saınchez, L. Vila, G. Desfonds. Nature Commun. **4**, 2944 (2013).
[9] Ye Du, S. Takahashi, J. Nitta. Phys. Rev. B **103**, 094419 (2021).
[10] T. Nan, T.J. Anderson, J. Gibbons. PNAS **116**, 16187 (2019).
[11] G.Y. Luo, J.G. Lin, Wen-Chung Chiang, Ching-Ray Chang. Sci. Rep. **7**, 6612 (2017).
[12] A.V. Khvalkovskiy, V. Cros, D. Apalkov. Phys. Rev. B **87**, 020402(R) (2013).

Publication of the Conference materials completed.